References

[1] Bjerknes, J. A. B., "Atmospheric Teleconnections from the Equatorial Pacific," to be published.

[2] Brinton, E., "Changes in the Distribution of Euphausiid Crustaceans in the Region of the California Current," CalCOFI Repts. VII, 1960.

[3] Emory, K. O., *The Sea Off Southern California, a Modern Habitat of Petroleum*, Wiley, New York, 1960.

[4] Hubbs, C. L., "Quaternary Paleoclimatology of the Pacific Coast of North America," CalCOFI Repts. VII, 1960.

[5] Jacobs, W. C., "The Energy Exchange between Sea and Atmosphere and Some of Its Consequences," *Bulletin Scripps Institution of Oceanography*, Vol. 6, 1951, University of California at Los Angeles, pp. 27–122.

[6] Lynch, H. B., "Rainfall and Stream Run-Off in Southern California since 1769," 1931, The Metropolitan Water District of Southern California.

[7] Masuzawa, J., "Statistical Characteristics of the Kuroshio Current," *Oceanographical Magazine*, Vol. 12, No. 1, 1960.

[8] McGowan, J. A., "Geographical Variation in *Limacina helicina* in the North Pacific," *Speciation in the Sea*, Publ. 5, 1963, Systematics Association.

[9] Namias, J., "Thirty Day Forecasting, a Review of a Ten Year Experiment," *Meteorological Monographs*, Vol. 2, No. 6, American Meteorological Society, Boston, Mass. 1953.

[10] Namias, J., "The Meteorological Picture 1957–1958," CalCOFI Repts. VII, 1960.

[11] Namias, J., "Short Period Climatic Fluctuations," *Science*, Vol. 147, No. 3659, 1965, pp. 696–706.

[12] Namias, J., "Macroscopic Association between Mean Monthly Sea-Surface Temperature and the Overlying Winds," *Journal of Geophysical Research*, Vol. 70, No. 10, 1965, p. 2307.

[13] Reid, J. L., "Oceanography of the Northeastern Pacific Ocean During the Last Ten Years," CalCOFI Repts. VII, 1960.

[14] Renner, J. A., "Sea-Surface Temperature Charts, Eastern Pacific Ocean," *California Fishery Market News Monthly Summary*, U.S. Dept. of the Interior, Bureau of Commercial Fisheries, Biological Lab., La Jolla, Calif.

[15] Roden, G. I. and Reid, J. L., "Sea Surface Temperature, Radiation, and Wind Anomalies in the North Pacific Ocean," *Records of Oceanographic Works in Japan*, Vol. 6, No. 1, 1961.

[16] Schell, I. I., "Dynamic Persistence and its Applications to Long-Range Foreshadowing," *Harvard Meteor Studies 8*, 1947.

[17] Soutar, A., "The Accumulation of Fish Debris in Certain California Coastal Sediments," CalCOFI Repts. XI, 1967.

[18] Takenouti, Y., "The 1957–1958 Oceanographic Changes in the Western Pacific," CalCOFI Repts. VII, 1960.

APRIL 1969 J. HYDRONAUTICS VOL. 3, NO. 2

Suspended Rigid Underwater Arrays

F. T. GEYLING*
Bell Telephone Laboratories Inc., Whippany, N. J.

The potential uses of large underwater arrays, supported in the sound channel without near field obstructions, have been of recurrent interest. This paper treats two proposed suspended array configurations designed to maintain a two- or three-dimensional matrix of transducers within given dimensional tolerances under normal environmental conditions. These tolerances result from a statistical analysis of array performance in response to structural deformations and random perturbations of the medium. One structure involves prestressing a network of suspension wires that hold the hydrophones in position; and the other uses an inflated envelope to protect the hydrophone array against the environment. The performance of critical components of each configuration is examined under static and dynamic loads. The behavior of each structure as a rigid body, held by its mooring lines, is investigated in some detail, including translational movement and attitude changes in response to steady and transient loads. For structures with a protective envelope, an acoustic analysis is required to assure tolerable effects at the hydrophones.

Nomenclature

a = membrane radius
c = speed of sound (in water)
k = wave number
$\bar{n}$ = direction of planar acoustic wave
$\bar{n}_0$ = steering vector of array
p_b = bouyancy force of flotation chambers; per unit area of membrane above mooring ring
p_γ = weight (in water) per unit area of membrane
p_i = internal pressurization of membrane
P_m = mooring force from anchor lines per unit length of mooring ring; assumed uniformly distributed
r = radial coordinate
u = transverse deflection of plane array
t = membrane thickness or time
E = Young's modulus
N = number of hydrophones
Ox_1, x_2, x_3 = rectangular Cartesian system
R = radius of spherical membrane
V = ambient current velocity
W_B = bouyancy force
$\Delta X_{\mu j}$ = differential position vector
α_i = amplitude parameter
β = angle between x_2 axis and incoming wave
γ = membrane density
$\delta\varphi_\mu$ = phase change of μth hydrophone response
λ = direction of ambient current in horizontal plane, or wavelength (evident from context)
σ = standard deviation
φ_e = external velocity potential
φ_i = internal velocity potential
ρ = density of water
Ω = characteristic frequency of a structure

Presented as Paper 68-477 at the AIAA 3rd Marine Systems and ASW Meeting and Technical Display, San Diego, Calif., April 29–May 1, 1968; submitted April 22, 1968; revision received October 23, 1968. The author acknowledges use of detailed calculations by F. K. Bogner, A. J. Claus, J. M. Gormally, A. G. Lubowe, R. Pringle, and D. A. Sonstegard on which the various sections were based. Some of their work, as listed in the references, will be documented more fully in separate publications.

* Head, Analytical Mechanics and Engineering Physics Department. Associate Fellow AIAA.

1. Introduction

RECENT underwater sound activity has included studies and speculations on potential uses of the sound channel for long-range transmission and reception of acoustic signals. Although several prognoses have been favorable, this possibility must be ultimately explored by experiments, some of which are under preparation. If they prove encouraging and have interesting system implications, there may be a need for structural assemblies to maintain highly directional arrays of hydrophones near the axis of the sound channel without surface flotation or bottom support.

Simple devices of this kind are in use: single moored lines forming vertical linear arrays and tripod moorings for single instrument packages (often referred to as "seaspiders"). Immediate extensions of these might be relatively flexible two-dimensional arrays of the "fish net" type, a neutrally buoyant pipe between two seaspiders supporting a horizontal linear array, and two-dimensional frames suspended similarly. Sizable underwater structures become extremely awkward, if not impossible, to manipulate unless they are at least neutrally buoyant. For this reason, conventional structural frame designs must be eliminated a priori.

In this paper we examine prestressing and inflation as schemes for achieving structural rigidity with minimum weight underwater. Examples have been chosen to explore areas of interest, such as structural stiffness, dynamic response, and acoustics. The proposed configurations seem acceptable from these points of view, but are beyond the practical state-of-the-art and may be an upper bound on the complexity of underwater technology for some time to come. Field trials, to advance their practicality, must resort to greatly simplified or scaled-down prototypes, as discussed in the final section.

The first structure studied consists of four compression members connected at a common joint, whose outer ends mark corners of a tetrahedron (Fig. 1). They are held in position by pretensioned cables, forming the edges of the tetrahedron. The structure is provided with buoyancy in the compression members or by separate flotation units (not shown) at the upper corners. This upward force enables it to be moored rigidly with three main lines to gravity anchors on the ocean bottom. Each anchor line is connected by three strands attached to the corners of one face of the tetrahedron. Each triangular face serves as a suspension frame for a network of high-strength cables that are pulled inward by a set of guy wires connected to the central joint of the structure. Each guy wire loads one node of the triangular net, thus helping to prestress it. Hydrophones mounted at these nodes form the acoustic array.

The second structure employs a pressurized spherical membrane (Fig. 2) to provide over-all rigidity and to prestress an internal system of steel cables suspended in a meridional section of the sphere. This supports a vertical array of hydrophones. The spherical envelope also protects the array from environmental forces, thus resembling a radome. The membrane is filled with sea water, both for convenience and for acoustic match. Internal pressure and some buoyancy are provided by an air pocket at the top. Additional buoyancy is provided by several compartments distributed over the polar cap of the sphere which are filled with a lighter-than-water liquid. The unit is moored to the ocean bottom by anchor lines connected to a mooring skirt that runs along a circle of latitude above the equatorial plane.

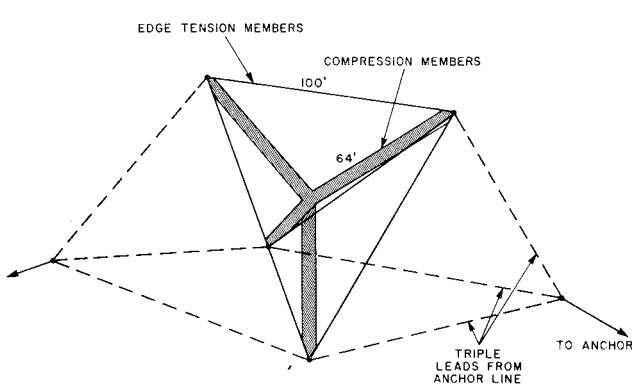

Fig. 1 Tetrahedral array (mooring lines from backface omitted for clarity).

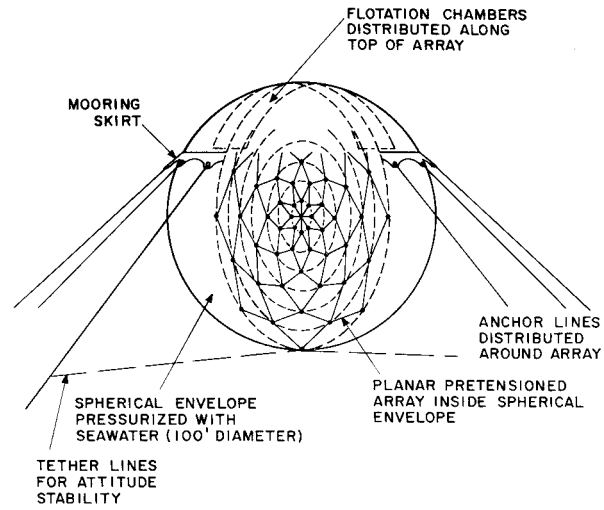

Fig. 2 Underwater radome.

Proceeding to the feasibility of the primary components of the two configurations, the spinal compression members for the tetrahedral array come close to current technology. They might be lattice columns assembled from modules with built-in flotation chambers or they could be individually deployed by mechanisms controlled from a surface vessel. While their basic feasibility is not a serious problem, the opposite is true of the over-all prestressing scheme proposed for the tetrahedron. Its response to steady drag forces from ambient currents and dynamic transients from the mooring system must be explored. Similar questions arise with the underwater radome of the second configuration, including its acoustic effects on the internal hydrophones. In both cases the feasibility of maintaining a fixed position and attitude for the entire structural unit by the proposed mooring system must be explored. Finally, since residual distortions of the array are unavoidable, their effects must be evaluated acoustically and compared with other acoustic degradations resulting from the ocean environment.

2. Prestressed Cable Nets

Internal prestressing has been widely accepted as a means of reducing structural weight and enhancing rigidity. Suspended arrays should be no exception. The principles involved in the tetrahedral array are three-dimensional extensions of prestressed cables.

Consider a string under uniform transverse load, which produces the well-known parabola. Suppose this load to be anticipated by a uniform distribution of transverse guy wires (Fig. 3), all stressed to the same level. When the actual load is applied, the prestress of the guy wires will relax. The amount that each wire shortens due to elastic recovery represents a deflection of the main cable, and is one or two orders of magnitude less than the cable deflections without prestressing. In practice the guy wires will converge to a limited number of suitable anchor points, and the prestressing system will be designed as a compromise between several environmental loads from various directions with different distributions.

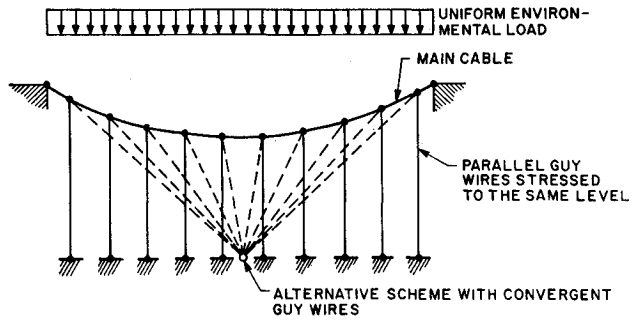

Fig. 3 Prestressing of single cable.

In studying the tetrahedral structure, consider a single quasi-triangular net whose corners are 100 ft apart and whose interaction with the remaining structure is ignored by specifying ad hoc kinematic constraints at the edges (Fig. 4). All prestressing guy wires are anchored at a point 20 ft behind the centroid of the triangle. The layout of members in the network is dictated by the desire to increase the density of nodes, and hence hydrophones, toward the center for acoustical reasons. Typical cable diameters for high-strength steel are 0.25 in. for the edge members, 0.10 in. for interior members, and 0.075 in. for guy wires. Each node is preloaded by a guy wire. For computational convenience, the drag loads are discretized to act also at these points, and estimated for a 1-knot current. The static analysis of such a structure follows standard methods for truss calculations, except that members that might ordinarily go into compression become slack and are dropped from the stiffness matrix.

Numerical results for this single-net structure under drag loading normal to the plane of the triangle show that deflections are about a foot without prestressing and fractions of an inch with prestressing. The significance of these slight deformations is decreased a little further because their homologous components are ignorable for acoustic purposes; i.e., each new node position should be compared with its counterpart on a parallel transposition of the unloaded, but prestressed, net made to coincide with the loaded shape at the center point (1 in Fig. 4).

To study the complete tetrahedral array, the artificial edge constraints for each net must be replaced by equilibrium and compatibility equations that connect it to adjacent nets. For simplicity, consider a current parallel to a plane of symmetry of the tetrahedron, thus involving one half of the front face and the adjacent side face. Suitable prestressing members are introduced between the edges of the top face, and deformations of the spinal compression members are taken into account. The iterative procedure required to meet all the governing conditions and to allow for slack members becomes involved, and care must be taken to assure numerical convergence. The technique is based on minimizing the potential energy of the structure.[1] Figures 5 and 6 show the structural geometry and the set of node displacements for the prestressing and current load previously given.

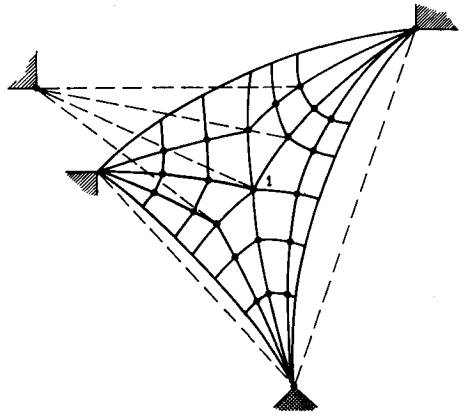

Fig. 4 Prestressed cable network.

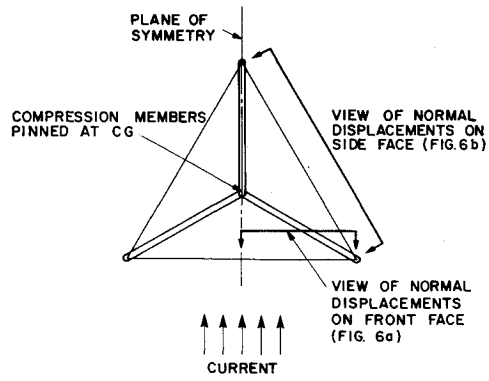

Fig. 5 Top view and load diagram for tetrahedral array.

Further studies should include the dynamic response of the prestressed tetrahedron. Although the attitude and mooring transients to be discussed in Sec. 4 will probably not affect the structure significantly, strumming of individual cables due to vortex shedding and its carryover to other cables and hydrophones is of concern. This effect may be mitigated by hydrodynamic spoilers on the cables and acoustic isolation of the hydrophones. A complete design study may also reveal that slackening of some members, in view of highly divergent directions and distributions of drag loading, is hard to avoid.

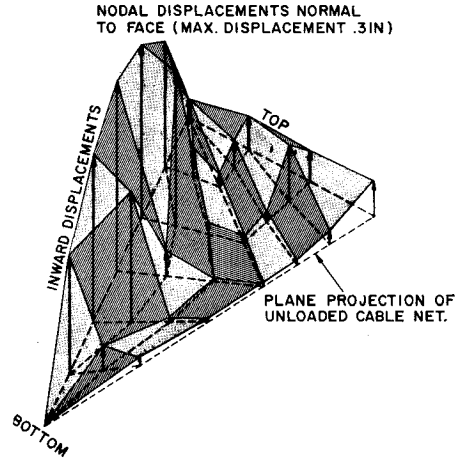

Fig. 6a Normal displacements on front face of prestressed tetrahedral array under 1-knot current.

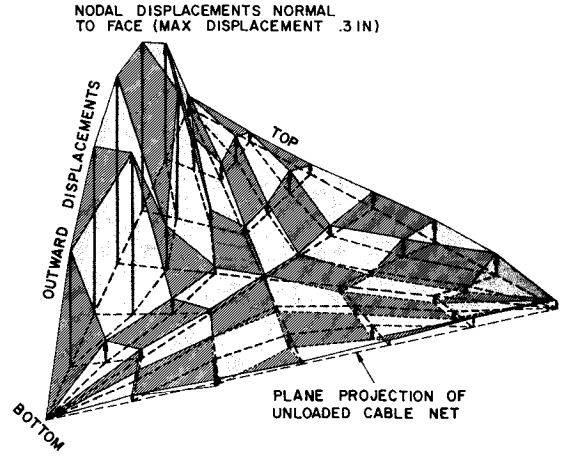

Fig. 6b Normal displacements on side face of prestressed tetrahedral array under 1-knot current.

This suggests that the tension in some of the guy wires be made adjustable from the center of the structure to maintain favorable stress conditions at all times.

3. Analysis of Inflated Membranes

In the second array configuration an inflated spherical envelope serves to rigidize the hydrophone supports, instead of prestressed guy wires. Thus, the deformation and internal stresses of the inflated membrane under environmental loads must be understood. Also, since it encloses the hydrophones, its acoustic effects are of interest. Practical problems of manufacturing and deploying a sizable balloon of this kind and of maintaining it against marine life are not discussed in this paper.

A. Structural Analysis

1. *Static response*

Static analysis of the inflated buoyant spherical membrane fastened to the mooring system of Fig. 2 involves standard application of membrane shell theory. The load system under normal conditions of deployment is shown schematically in Fig. 7. Superposed on this pattern are pressures due to the ambient current, modeled as potential flow for simplicity.

Boundary conditions are derived from the need to avoid singularities at the poles, invariance of the enclosed volume under the action of external currents, and compatibility of meridional displacements across the mooring ring. In the last instance a discontinuity in the normal displacements could be tolerated by the usual argument that bending theory eliminates these by localized effects. In all of the foregoing, the inflative pressure p_i is used as an adjustable parameter to avoid compressive membrane stresses, which mean a slackening of the envelope. The following data were used in the analysis:

a = 50 ft, membrane radius
t = 0.25 in., membrane thickness
γ = 70 lbs/ft^3, membrane density
V = 1 knot, ambient current
W_B = 20,000 lbs, buoyancy force
E = 10^5 psi, Young's modulus for membrane
p_i = 0.1 psi

Figure 8 shows the radial displacement w in vertical planes normal and parallel to the current. In neither case does w become negative, which augurs well for keeping the internal hydrophone suspension under stress. The maximum value of w = 1 in., the moderate internal pressure of 0.1 psi required to prestress the membrane, and the relatively small membrane stresses (in the order of 100 psi) make this structure sufficiently promising for a detailed study.[2] Obvious study refinements include a more realistic pressure distribution and nonuniform mooring forces P_m due to ambient currents, deformations of the mooring ring, and the effect on the membrane of inextensible internal hydrophone suspension cables.

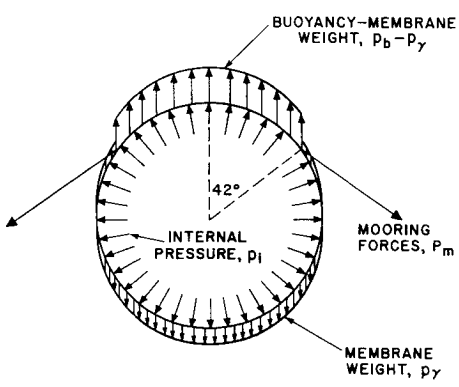

Fig. 7 Static loading on underwater radome.

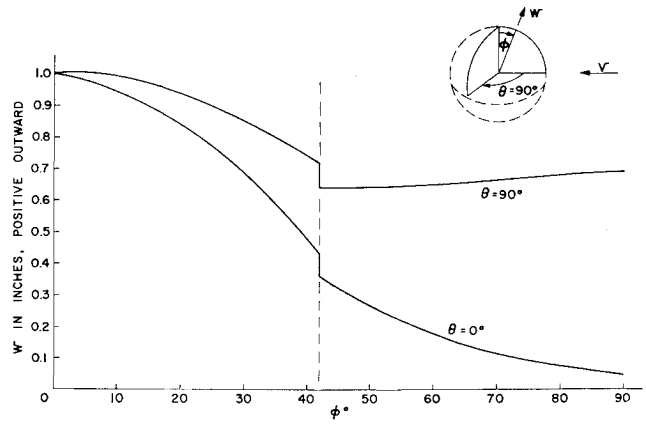

Fig. 8 Radial displacements of inflated membrane under mooring loads and a 1-knot current.

2. *Dynamic response*

Free vibrations of the inflated envelope may be analyzed by treating the surrounding fluid as incompressible and considering only the membrane behavior of the structure. While the latter assumption may be justifiable, the former is questionable, since it amounts to the requirement that $\Omega R \ll c$, where Ω = any one of the participating characteristic frequencies of the structure. Although the lowest structural modes are usually the most strongly excited ones, at some of the higher vibration modes (which still come into play) this inequality does not hold. Thus, the free response was analyzed for both types of media, with and without bending effects in the shell.[3]

The calculations are based on an energy method of the Rayleigh-Ritz type. The shell displacement components are developed in Legendre series of the meridional angle with time-dependent coefficients, and the potential and kinetic energies of the shell follow from standard expressions. In the incompressible case, ϕ_i and ϕ_e (which are governed by Laplace's equation in this case) are also written as Legendre series. The kinetic energy of the moving fluid is expressed in terms of ϕ and $\partial\phi/\partial r$ at the membrane by use of one of Green's identities. For the compressible case a Legendre series solution of the wave equation is used for the velocity potential, and the dynamic pressure on the shell follows from $p = -\rho(\partial\phi/\partial t)$, where ρ is approximately the static fluid density. This surface pressure enters into the calculation of generalized forces for the equations of motion. In both the incompressible and compressible case, these equations are generated from the Lagrangian, and ultimately reduce to equations for the modal amplitude functions.

Examination of the numerical results in Ref. 3 shows that the fluid interaction significantly reduces the frequencies of the shell modes that contain bending effects, and changes the character of membrane modes from combined radial and meridional displacements to predominantly meridional ones without affecting their frequencies appreciably. The sensitivity of this effect to compressibility of the fluid deserves notice. The most significant outcome of these studies is the estimate of structural response to transient loading. Thus, in the case of a nearby detonation, the largest part of the energy impinging on the membrane seems to transfer to the internal fluid (as suggested by the acoustic attenuations calculated below). A simplified impulse calculation establishes initial conditions for membrane response to blast loading through an incompressible fluid. Thus, 300 lb of TNT exploded 50 ft from a 100-ft envelope produces momentary deflections of about 1 in. and stress levels of about 2000 psi.

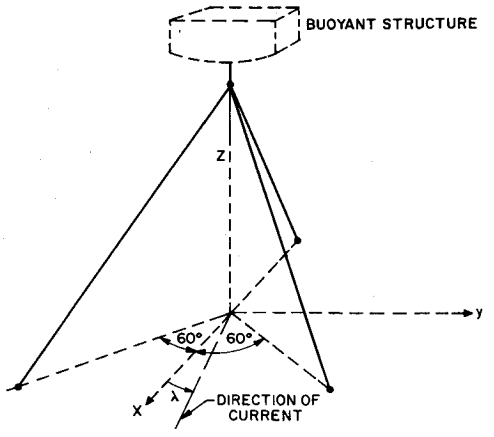

Fig. 9 Tripod mooring.

These effects of a detonation seem harmless and become insignificant at 200 ft from the source. This result does not, however, predict how electro-acoustic instrumentation inside the sphere will fare under such blast loading.

B. Acoustic Performance

Aside from the reduction of the received signal due to acoustic energy retained by the membrane, phase distortions imposed on interior waves are of interest. The first part of our acoustical study[2] concerns local transmission phenomena, based on a classical study[4] of transmission through a plane, elastic, immersed layer. For the material constants given, negligible attenuation and phase shift of the transmitted wave are predicted, except for three critical arrival angles of the incident wave. At the largest of these the dilatation mode in the solid reduces to surface waves along the insonified face of the elastic sheet. At the next angle the transmitted wave amplitude drops sharply and practically all the acoustic energy is reflected back against the incident wave. At the third angle the shear mode reduces to surface waves. In each case the dilatation and/or shear waves in the solid attain large amplitudes, involving sizeable but tolerable stresses. Since a spherical envelope exposed to a plane wave will localize these critical incidence phenomena along discrete minor circles, they are deemed to be unimportant.

The acoustic performance of a spherical envelope may be estimated by superposing local transmission effects based on the previous approach. A more exact treatment is obtained by solving the wave equation in spherical coordinates in terms of Legendre-Bessel series. They involve the usual manipulations and computations to evaluate coefficients from boundary conditions,[5] and predict innocuous acoustic effects, as anticipated. For steady excitation, the phase distortions in a great-circle plane parallel to the incident wave front is within

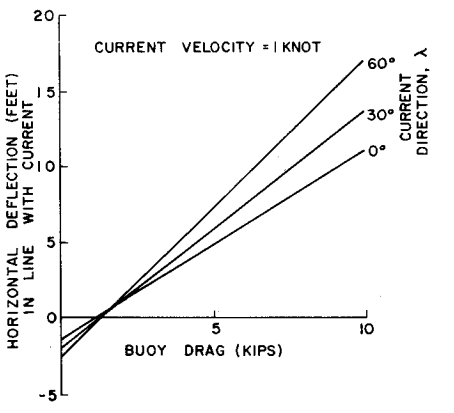

Fig. 10 Deflection at apex vs buoy drag.

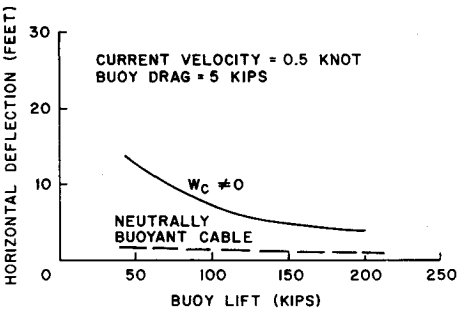

Fig. 11 Horizontal deflection vs buoy lift for different cable weights.

0.1° for $\frac{2}{3}$ of the radius and below 1° for the remainder. Similarly, amplitude distortions are negligible, except for a few points in the back half of the spherical cavity where an amplification of 10% may occur due to focusing of reflections from the back wall. These could be suppressed by an absorbent coating on that wall if hydrophones are to be suspended in more than one meridional plane to increase the horizontal view of the array. The only acoustical problem remaining is flow noise from the turbulent boundary-layer outside the envelope. Presumably, its spectrum will become known and may be discriminated against.

All in all, the inflated spherical membrane is a promising candidate as an underwater radome, because of virtual immunity of array geometry to environmental forces. The price one pays is a heavy mooring system and reduced accessibility of the hydrophones. If the latter is objectionable, the instrumentation may be placed outside the membrane, resulting in a spherical array geometry and a somewhat increased sensitivity to environmental forces.

4. Mooring Systems

A. Translational Motion

Common to all mooring systems is a system of buoyancy forces that prestress the anchor lines. Other loads are mostly current forces, though occasional interference from mudflow on the ocean bottom, from trawlers, and (for shallow installations) from exceptional tidal waves may occur.

The well-known tripod, or "seaspider," moorings may be extended for this application. Consider the tetrahedral structure instead of a single buoy at the vertex. An anchor line is assigned to each of the triangular faces, as shown in Fig. 1. With the underwater radome, a mooring skirt is provided where anchor lines are attached.

The analysis of multi-cable systems proceeds from the stress-deflection analysis of single cables. For dead-weight

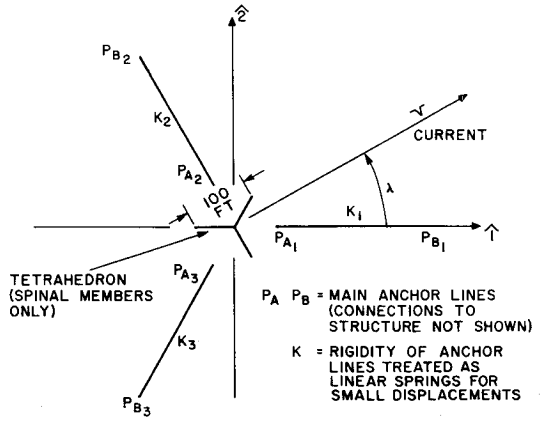

Fig. 12 Plan view of mooring system for tetrahedral array.

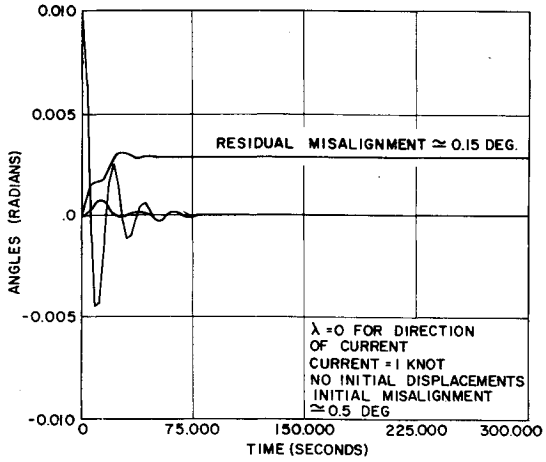

Fig. 13 Attitude perturbations for tetrahedral array against time.

loading this is the well-known catenary. For more general load distributions derivable from various current profiles as a function of depth, series solutions are used, as convenient.[6] The significant results of this analysis are the maximum cable tension, the terminal forces, and the sensitivity of these quantities to displacement of the cable ends, current velocity, and cable weight in water. The force-displacement relations at the ends of each single cable are needed to determine the equilibrium and compatibility equations for each joint in a multi-cable system.

A few characteristics of tripod mooring systems apply regardless of whether a simple buoy or, for example, a tetrahedral structure is located at the vertex. Figure 9 shows such a system. Figure 10 shows its horizontal buoy displacement vs buoy drag and current direction, for a current of 1 knot. The interesting feature shown is an "upstream" shift of the buoy for small buoy drag, due to sag in the upstream cable caused by current forces. This effect disappears for large drag forces on the buoy. The cable weight in water is important as shown in Fig. 11. The mooring system tightens against horizontal displacement with increasing buoy lift if the cables are heavier than water, and this effect all but disappears for neutrally buoyant cables.

A straightforward extension of these studies accommodates situations, such as Fig. 2, where numerous cables are attached to a mooring skirt. However, the actual number and sizes of cables required to secure an underwater radome against large drag forces raise important practical difficulties. A typical design might involve ten 0.5-in. steel cables for a 100-ft inflated membrane.

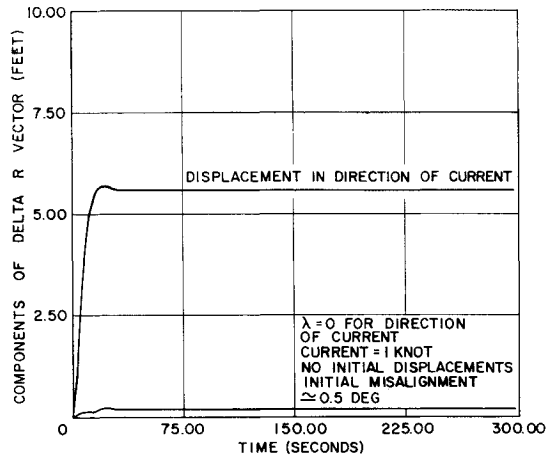

Fig. 14 Displacement of tetrahedral array against time.

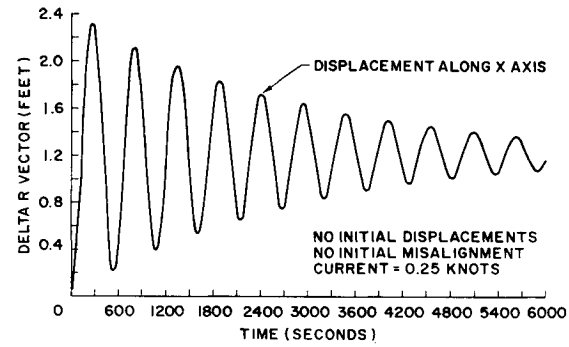

Fig. 15 Displacement in the direction of current against time for underwater radome.

B. Attitude Motion

Once a large object is placed at the vertex of a mooring system, its rigid body motion becomes of interest and it is usually coupled with the translational response to current loading. Analyses for attitude dynamics of suspended arrays and a rather complete set of results are given in Ref. 6. Equations of translational and rotational motion were developed in vector notation, using the drag formulas and force-displacement relations of individual anchor lines employed in the tripod analysis. A plan view of the moorings for a tetrahedral structure is given in Fig. 12, for a height of 8000 ft above the ocean floor of the over-all tripod. The anchor lines run from P_B to P_A opposite each face of the tetrahedron, and the direction of the current is given by λ. Typical results from a digital computer are shown in Figs. 13 and 14 for an initial angular displacement of 0.01 rad and a step function in the current of 1 knot. Although this form of excitation is idealized and somewhat exaggerated, it is indicative of structural recovery from changes in ambient current or trawler interference. The settling time is less than a minute, with negligible residual misalignment.

The underwater radome of Fig. 2 was similarly studied. Typical dimensions and forces resemble those of Sec. 3, and ten mooring lines were assumed. Additional tether lines from the main anchor cables to the lower pole of the sphere are essential for attitude stability. Figures 15 and 16 indicate the dynamic response to a change in current. The governing characteristic is a long translatory period, due to mass and drag of the balloon, and a very rapid attitude response. Residual rotations due to a quarterknot change of current are in the order of $\frac{1}{2}°$. This may be acoustically significant but could be acceptable in view of conservative assumptions used for this analysis. As in Sec. 3, deformations of the mooring ring were neglected. Similarly, the drag loads on

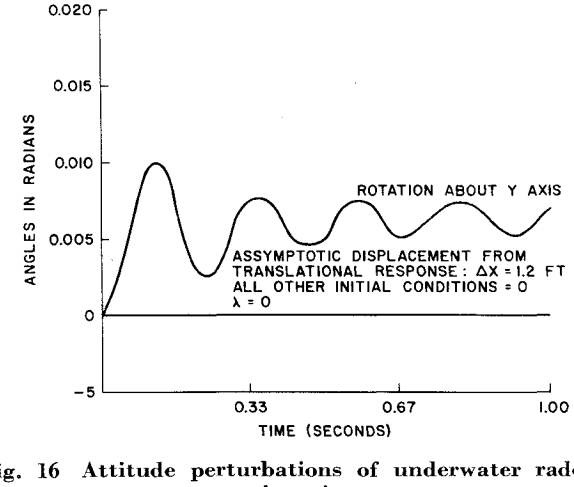

Fig. 16 Attitude perturbations of underwater radome against time.

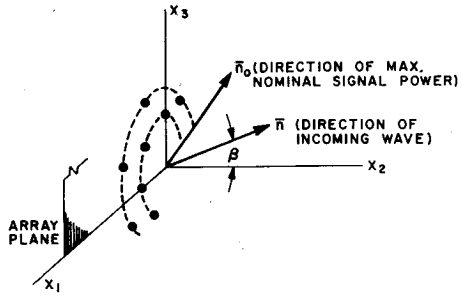

Fig. 17 Layout of planar array (within underwater radome).

the anchor lines, which are probably of secondary importance, were ignored.

5. Acoustic Array Performance

No structural scheme guarantees against array distortions. Unusual load conditions may cause some hydrophone suspensions to "go slack," at least temporarily. Thus, it is necessary to assess the effects of hydrophone displacements on acoustic array performance in order to develop meaningful structural design criteria or to compensate for array distortions during acoustical-data processing. One way to provide such appraisals is in terms of modal functions for the structural deformations and to relate the statistics of their amplitude coefficients to those of acoustical parameters, such as gain, beam width, and side lobe suppression.

Considered here is the effect of structural deformations on the beam pattern of the array of Fig. 2. The deflection of the hydrophone plane is assumed to consist of a linear combination of a number of deflection modes, taken in the form $\cos(i - \frac{1}{2})\pi r/R$, where r measures distance from the center and R is the radius of the enclosing radome. The deflection of the supporting plane is

$$u = \sum_{i=1}^{M} \alpha_i \cos\left(i - \frac{1}{2}\right)\frac{\pi r}{R}$$

Here, the α_i are considered normally and independently distributed random variables with zero mean and variance σ^2, which is chosen to reflect realistic deformations. Studied below is the beam pattern for a range of values of σ expressed in wavelengths of the received signal.

In Fig. 17, $Ox_1x_2x_3$ is a rectangular Cartesian system with horizontal plane Ox_1x_2. The vertical plane Ox_1x_3 is the plane of the (undisturbed) array. The unit vector $\bar{n}$ specifies the direction of the incoming wave, and $\bar{n}_0$ is any unit vector to which the array is steered.

If the hydrophone responses are equally weighted, the ratio G of array signal power for any $\bar{n}$ to maximum signal power is

$$G = \frac{1}{N^2}\sum_{\mu=1}^{N}\sum_{j=1}^{N} \cos[k\Delta X_{\mu j}\cdot(\bar{n}_0 - \bar{n}) + \delta\phi_\mu - \delta\phi_j] \quad (1)$$

where $\Delta X_{\mu j}$ is the difference in position vectors of the μth and jth hydrophone, and $\delta\phi_\mu$ is the phase change of the response of the μth hydrophone caused by the displacement of the supporting net. If the hydrophone displacements are orthogonal to the supporting plane, the phase variations are

$$\delta\phi_\mu = k\cos\beta \sum_{i=1}^{M} \alpha_i \cos\left(i - \frac{1}{2}\right)\frac{\pi r_\mu}{R} \quad (2)$$

The effect of structural deformations is studied by taking expected values on both sides of (1), thereby obtaining an "expected beam pattern." One finds

$$E\{G\} = \frac{1}{N^2}\sum_{\mu=1}^{N}\sum_{j=1}^{N} e^{-\frac{1}{2}\,\mathrm{var}\,[\delta\phi_\mu - \delta\phi_j]}\,[\cos k\Delta X_{\mu j}\cdot(\bar{n}_0 - \bar{n})] \quad (3)$$

where the variance of $\delta\phi_\mu - \delta\phi_j$ follows from (2);

$$\mathrm{var}\{\delta\phi_\mu - \delta\phi_j\} = k^2\sigma^2\cos^2\beta \sum_{i=1}^{M}\left[\cos\left(i - \frac{1}{2}\right)\frac{\pi r_\mu}{R} - \cos\left(i - \frac{1}{2}\right)\frac{\pi r_j}{R}\right]^2$$

Clearly, for $\partial = 0$, (3) produces the exact beam pattern, i.e., the pattern in the absence of structural deformations.

Equation (3) was used to study the acoustical behavior of the array suspended in the sound channel as indicated in Fig. 18. The array receives a continuous wave originating 130 miles away. Since the hydrophones are mounted with circular symmetry, the vertical and horizontal beam patterns are the same for zero scan angles. The vertical scan angle for the wave shown in Fig. 18 is about 10° and the horizontal scan angle is taken equal to zero. The vertical and horizontal beam patterns are then so close that only one must be displayed.

Figures 19 and 20 show the exact beam pattern for a radome radius of 20 wavelengths (say 50 ft), and expected patterns for various values of ∂/λ. Results of Fig. 19 correspond to one deflection mode. As expected, the on-axis gain is reduced while the nulls in the beam pattern are being smoothed out. Elimination of nulls is more pronounced than loss of on-axis gain, primarily because the former is a first-order effect of phase fluctuations whereas the latter is second order.

Figure 20 compares two expected beam patterns from one deflection mode and from ten modes, respectively. The standard deviations of displacements at the center were taken to be half a wavelength in both cases. The more irregular

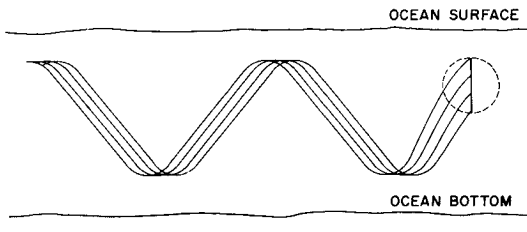

Fig. 18 Propagation pattern for array sensitivity study (vertical scale exaggerated).

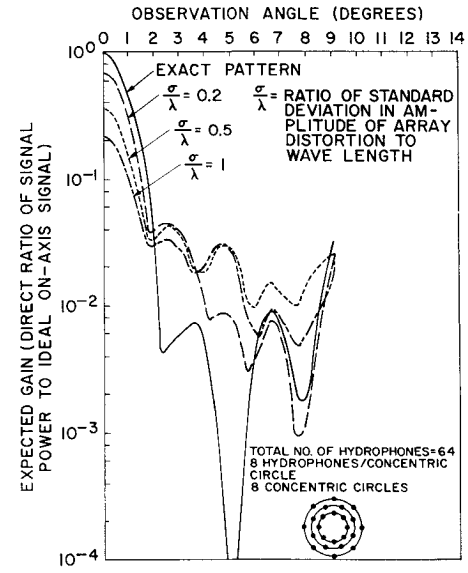

Fig. 19 Beam patterns of planar array under single-mode distortions.

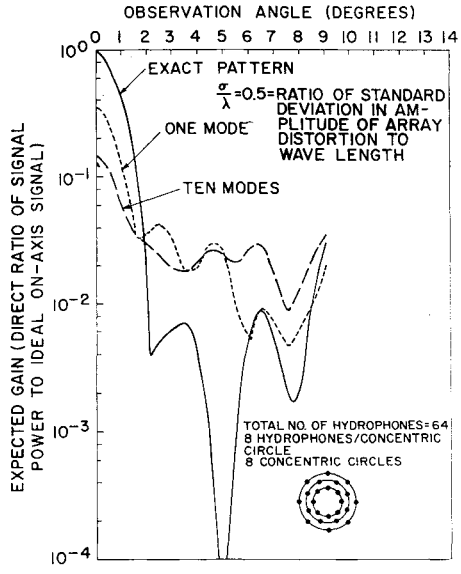

Fig. 20 Beam patterns of planar array under single-and multi-mode distortions.

deflection pattern corresponding to ten modes results in a further deterioration of the beam.

The modal approach used in this computation of beam patterns is of value in case the actual deformations are represented satisfactorily with a truncated (Fourier) series containing few terms. For the displacement patterns of the tetrahedral array (Fig. 6) this is quite unlikely. Instead, one may use displacement vectors at each node (i.e., each hydrophone) with a suitable modification of Eq. (3). Further details on array sensitivity studies are given in Refs. 7 and 8.

6. Conclusions

This paper discusses the fundamentals of prestressed, inflatable array structures and suggests solutions based on theoretical analyses. Several technological problems, however, require attention, including, for example, miniaturized underwater instrumentation (hydrophones, preamplifiers, multiplexers, electrical cabling, power sources) to minimize the inert weight of the suspended structure[9] as well as the means for successful deployment. Established techniques, involving surface vessels, and new ones, using underwater manipulators, will have to be further developed before the assemblies suggested can become practical. This includes calibration procedures to identify acoustical biases from structural misalignment during installation. Finally there is the need to protect the underwater installations from destructive influences of the ocean environment. Here the inflatable underwater radome presents special materials problems.

There is a tradeoff between structural refinement and other forms of sophistication. Rather than seeking a maximum of structural rigidity, one may monitor the deformations that occur. These, then, may be countered by "trimming" the structure or by compensations in the acoustical-data processing. The approach to be taken depends not only on technical considerations but also on operational aspects and system implications.

References

[1] Bogner, F. K., "Applications of Potential Search Methods to Prestressed Underwater Arrays," Bell Telephone Lab., Whippany, N. J.

[2] Loutzenheiser, C. B., Lubowe, A. G., and Sonstegard, D. A., "The Acoustic and Structural Characteristics of Undersea Radomes," TR 15, Dec. 1966, U.S. Navy Contract N0014-66-C0005.

[3] Sonstegard, D. A., "Effects of a Surrounding Fluid on the Free, Axisymmetric Vibrations of Thin Elastic Spherical Shells," *The Journal of the Acoustical Society of America*, Vol. 45, No. 2, Feb. 1969, pp. 506–510.

[4] Reissner, H., "Der senkrechte und schräge Durchtritt einer in einem flüssigen Medium erzeugten ebenen Dilatations-(Longitudinal)–Welle durch eine in diesem Medium befindliche planparallele feste Platte," *Helvetica Physica Acta*, Vol. 11, 1938, p. 140, erratum p. 268.

[5] Goodman, R. R. and Stern, R., "Reflection and Transmission of Sound by Elastic Spherical Shells," *The Journal of the Acoustical Society of America*, Vol. 34, No. 3, March 1962, p. 338.

[6] Gormally, J. M. and Pringle, R., "Analysis of Mooring Systems and Rigid Body Dynamics for Suspended Structures," TR 14, Dec. 1966, U.S. Navy Contract N0014-66-C0005.

[7] Claus, A. J. and Pringle, R., "Sensitivity Studies of Acoustic Arrays," TR 16, Dec. 1966, U.S. Navy Contract N0014-66-C0005.

[8] Claus, A. J., "Propagation of Sound Pulses in a Randoni Medium with Variable Mean Refraction Index," TR 21, Dec. 1967, U.S. Navy Contract N 0014-66-C0005.

[9] Buus, R. G. et al., "State-of-the-Art and Feasibility Studies for Underwater Instrumentation," (U)TR 17 (Conf.), Dec. 1966, U.S. Navy Contract N0014-66-C0005.